Revised es-2008-3357b.R2

Supporting Information for

Effects of Copper, Lead and Cadmium on the Sorption of 2,4,6-trichlorophenol onto and Desorption from Wheat Ash and Two Commercial Humic Acids

YU-SHENG WANG,[†] XIAO-QUAN SHAN,[*,†] MU-HUA FENG,[* †,‡] GUANG-CAI CHEN,[†,§] ZHI-GUO PEI,[†] BEI WEN[†], TAO LIU,[⊥] YA-NING XIE,[⊥] AND GARY OWENS[∥]

[†]State Key Laboratory of Environmental Chemistry and Ecotoxicology, Research Center for Eco-Environmental Sciences, PO Box 2871, Beijing 100085, China,

[‡]State Key Laboratory of Lake Science and Environment, Nanjing Institute of Geography and Limnology, Chinese Academy of Sciences, 73 East Beijing Road, Nanjing 210008, China,

[§]Research Institute of Subtropical Forestry, Chinese Academy of Forestry, Fuyang, Zhejiang 311400, China,

[⊥]Beijing Synchrotron Radiation Laboratory, Institute of High Energy Physics, Chinese Academy of Sciences, Beijing 100049, China, and

[∥]Centre for Environmental Risk Assessment and Remediation, University of South Australia, Mawson Lakes, SA 5095, Australia

*Corresponding author phone: +86-10-62923560; fax: +86-10-62923563;

E-mail: xiaoquan@rcees.ac.cn; mhfeng@niglas.ac.cn

21 Number of pages: 16

22 Number of tables: 3

23 Number of figures: 7

CPMAS ^{13}C NMR measurement

Solid-state ^{13}C NMR data were acquired using cross-polarization and magic angle spinning (CPMAS) on a 300-MHz NMR spectrometer (Varian, San Francisco, USA). Spectra were acquired at a frequency of 75 MHz with a ^{13}C MAS spinning rate of 13 kHz, contact time of 2 ms, 1 s recycle delay. The number of scans ranged from 5000 to 10000 per sample.

FTIR measurement

Fourier Transform Infrared (FTIR) spectra were obtained on a NEXUS 670 spectrophotometer equipped with deuterated triglycine (DTGS) and mercury-cadmium-telluride (MCT) detector, a KBr beam splitter and a sample bench purged with dry air. The resolution for FTIR spectra was 2.0 cm^{-1}, and a total of 64 scans were collected for each spectrum. The sample was prepared using the same conditions as were used for the sorption experiments. The initial solution concentration of TCP was 370 mg L^{-1}. The aqueous suspensions, containing TCP sorbed to ash or HA, were passed through a 0.45 μm hydrophilic polyethersulfone membrane on a Millipore holder. The resulting TCP sorbed samples deposited on the filter were allowed to air-dry overnight and were removed from the filter by running the filter and deposit over a knife edge. The FTIR spectra were recorded on pellets obtained by pressing a mixture of ash or HA (1 mg) with dried KBr (100 mg) under reduced pressure.

X-ray absorption measurements and data analyses

X-ray absorption spectra at Cu K-edges and Pb L_{III}-edges were recorded at a wiggler beamline and XAFS end station of Beijing Synchrotron Radiation Facility (BSRF) using a Si (111) double crystal monochromator. During the experiment, the storage ring was operating at 2.2 GeV with a beam current of ~80 mA. To suppress the unwanted high order harmonics, the parallism of the two crystals in the monochromator was adjusted to mistune the incident beam by 30%. The incident beam intensities were monitored and recorded using a nitrogen-15% argon gas flowing ionization chamber. The fluorescence signals were measured using Lytle-type detector (EXAFS Company, Pioche, NV, USA) with filter (EXAFS Materials Inc., Danvalle, CA, USA). XAS data were collected in an energy range from 8920 to 9080 eV for Cu and 12920 to 14000 eV for Pb, covering K-edge absorption of Cu atoms and the L_{III}-edge absorption of Pb atoms. Three scans were averaged for both adsorbed samples and chemical standards.

The code, WinXAS2.1, was used for data analysis (*1*). The mid-point of the absorption jump was chosen as the energy threshold. The pre-edge absorption background was fitted and subtracted using the Victoreen formula. The post-edge absorption backgrounds were fitted using the spline function and subtracted from the absorption spectra. The EXAFS functions were normalized using the absorption edge jump and were Fourier transformed to R-space with k^3-weighting over the range from 2.2−8.5 Å for Cu and 2−11 Å for Pb. The fit was performed in k-space with a model of one shell, where the coordination number (N), the atomic distance (R), energy offset (E0) and Debye-Waller factor (σ^2) were allowed to float freely. Phase shifts and

backscattering amplitudes were obtained from the theoretical calculation using FEFF6.0 (*2*) and fit with the reference compounds, $Cu(CH_3COO)_2$ and $Pb(CH_3COO)_2$.

Fluorescence Quenching Experiment

A 0.02 M pyrene stock solution was prepared in ethanol and diluted aqueous pyrene solutions (1×10^{-7} M) were prepared by placing the appropriate amount of stock solution in a dry volumetric flask and evaporating the ethanol. Subsequently, water was added and the solution was sonicated for at least 5 hrs. All working pyrene solutions were stored in the dark in glass flasks at room temperature. Quenching of pyrene fluorescence by bromide was measured by adding consecutive aliquots of 0, 0.04, 0.08, and 0.16 M KBr, respectively, to fluorescence-free quartz cavetti containing 5×10^{-8} M pyrene and 0, 10, and 20 mg L^{-1} ash or HA. After the addition of KBr the solution was allowed to equilibrate for at least 5 min before fluorescence measurement. An equilibration time of 20 min produced no significant change in fluorescence intensity. Adsorption of pyrene to the quartz cell walls was not detected. Fluorescence excitation was set at 240 nm, and the emission was measured at 373 nm (F-3000 fluorescence spectrophotometer, Hitachi Co., Japan). The background fluorescence of ash and HA was corrected. The fluorescence quenching experiment was repeated three times.

UV-Visible detection of pyrene

The concentration of pyrene was determined using a Hewlett-Packard Model 1100 gradient HPLC system equipped with an auto-injector, photodiode-array UV-Visible detector at 254 nm, and an extended polar selectivity reversed-phase column (15 cm × 4.6 mm i.d.). The mobile phase was a mixture of methanol and water (90:10) with a flow rate of 1.0 ml min^{-1}.

Literature cited

(1) Ressler, T. WinXAS: a new software package not only for the analysis of energy-dispersive XAS data. *J. Physique IV* **1997**. *7 (C2)*, 269−270.

(2) Zabinsky, S.; Rehr, J.; Ankudinov, A.; Albers, R.; Eller, M. Multiple scattering calculations of X-ray-absorption spectra. *Phys. Rev. B* **1995**. *52*, 2995−3009.

100

Table S1. Characteristics of Wheat ash, TJHA and GeHA

		ash	TJHA	GeHA
Ash (%)		1.66	9.16	6.56
C (%)		77.0	57.4	48.5
N (%)		0.56	1.72	1.07
H (%)		2.58	3.43	3.72
O (%)		18.2	28.3	40.2
H/C		0.40	0.71	0.91
O/C		0.18	0.37	0.62
N/C		0.01	0.03	0.02
(N+O)/C		0.19	0.40	0.64
BET Surface area (m^2 g^{-1})	No solutes adsorbed	410	36.7	32.6
	TCP-adsorbed	331	23.5	25.4
	Cu-adsorbed	369	27.6	24.2
	Pb-adsorbed	353	20.8	26.1
Alkyl C (0 - 50 ppm) (%)		8.9	11	41
O-alkyl C (50 - 110 ppm) (%)		6.9	16	42
Aromatic C (110 - 145 ppm) (%)		73	71	12
O-aryl C (145 - 163 ppm) (%)		9.0	1.0	1.2
Carboxyl C (163 - 190 ppm) (%)		2.6	1.0	3.4
Aliphatic C (%)		7.2	27	83
Aromatic C (%)		90	72	13
Aromaticity		12.5	2.66	0.16
Aliphaticity		0.08	0.38	6.26
*POC		0.182	0.177	0.466

*POC: percentage of polar organic carbon, was calculated from the peak areas listed

101

TABLE S2. Results of Freundlich Model Fitting to the Adsorption Isotherms for TCP.

		K_F	N	MWSE	R^2
ash	TCP alone	22.09 ± 1.25	0.40 ± 0.01	0.0072	0.994
	+ 0.1 mM Cd	21.20 ± 1.28	0.40 ± 0.01	0.0084	0.995
	+ 0.1 mM Cu	18.38 ± 0.20	0.38 ± 0.02	0.0061	0.995
	+ 0.1 mM Pb	18.29 ± 1.43	0.36 ± 0.01	0.0056	0.976
TJHA	TCP alone	1.50 ± 0.04	0.63 ± 0.01	0.0007	0.991
	+ 0.1 mM Cd	1.51 ± 0.06	0.63 ± 0.01	0.0014	0.989
	+ 0.1 mM Cu	1.25 ± 0.08	0.62 ± 0.01	0.0010	0.998
	+ 0.1 mM Pb	1.22 ± 0.09	0.61 ± 0.02	0.0028	0.987
GeHA	TCP alone	1.05 ± 0.10	0.79 ± 0.02	0.0900	0.988
	+ 0.1 mM Cd	1.09 ± 0.08	0.80 ± 0.02	0.0024	0.989
	+ 0.1 mM Cu	0.96 ± 0.04	0.79 ± 0.01	0.0032	0.983
	+ 0.1 mM Pb	0.99 ± 0.12	0.78 ± 0.02	0.0030	9.979

MWSE is the mean weighted square error, equal to $1/v \sum[(q_{measured}-q_{model})^2/q^2_{measured}]$, where v is the amount of freedom; $v=n-2$ for Freundlich Model; $n=18$ for ash, and 30 for TJHA and GeHA.

TABLE S3. XAFS Results of Metal Adsorbed Samples and Metal Reference Compounds

	neighboring atoms	R (Å)[a]	CN[b]	□σ² (Å²)[c]
$Cu(CH_3COO)_2$	$Cu\text{-}O_{eq}$	1.97	4.75	0.007
	$Cu\text{-}O_{ax}$	2.27	2.21	0.001
Cu^{2+} (aq)	$Cu\text{-}O_{eq}$	1.95	4.75	0.008
	$Cu\text{-}O_{ax}$	2.35	1.76	0.005
$Cu(OH)_2$	$Cu\text{-}O_{eq}$	1.95	3.85	0.005
	$Cu\text{-}O_{ax}$	2.52	2.09	0.008
CuO	$Cu\text{-}O_{eq}$	1.92	4.98	0.010
	$Cu\text{-}O_{ax}$	2.63	1.90	0.009
Cu^{2+} adsorbed-ash	$Cu\text{-}O_{eq}$	1.97	4.43	0.008
	$Cu\text{-}O_{ax}$	2.25	2.32	0.009
Cu^{2+} adsorbed-TJHA	$Cu\text{-}O_{eq}$	1.96	4.84	0.009
	$Cu\text{-}O_{ax}$	2.24	1.95	0.008
Cu^{2+} adsorbed-GeHA	$Cu\text{-}O_{eq}$	1.96	4.65	0.009
	$Cu\text{-}O_{ax}$	2.25	2.12	0.010
$Pb(CH_3COO)_2$	Pb-O	2.38	1.69	0.010
Pb^{2+} (aq)	Pb-O	2.48	2.75	0.010
PbO	Pb-O	2.31	3.92	0.009
Pb^{2+} adsorbed-ash	Pb-O	2.38	1.78	0.010
Pb^{2+} adsorbed-TJHA	Pb-O	2.38	1.80	0.009
Pb^{2+} adsorbed-GeHA	Pb-O	2.38	1.88	0.010

[a] Interatomic distance. [b] Coordination number. [c] Debye-Waller factor (Å²).

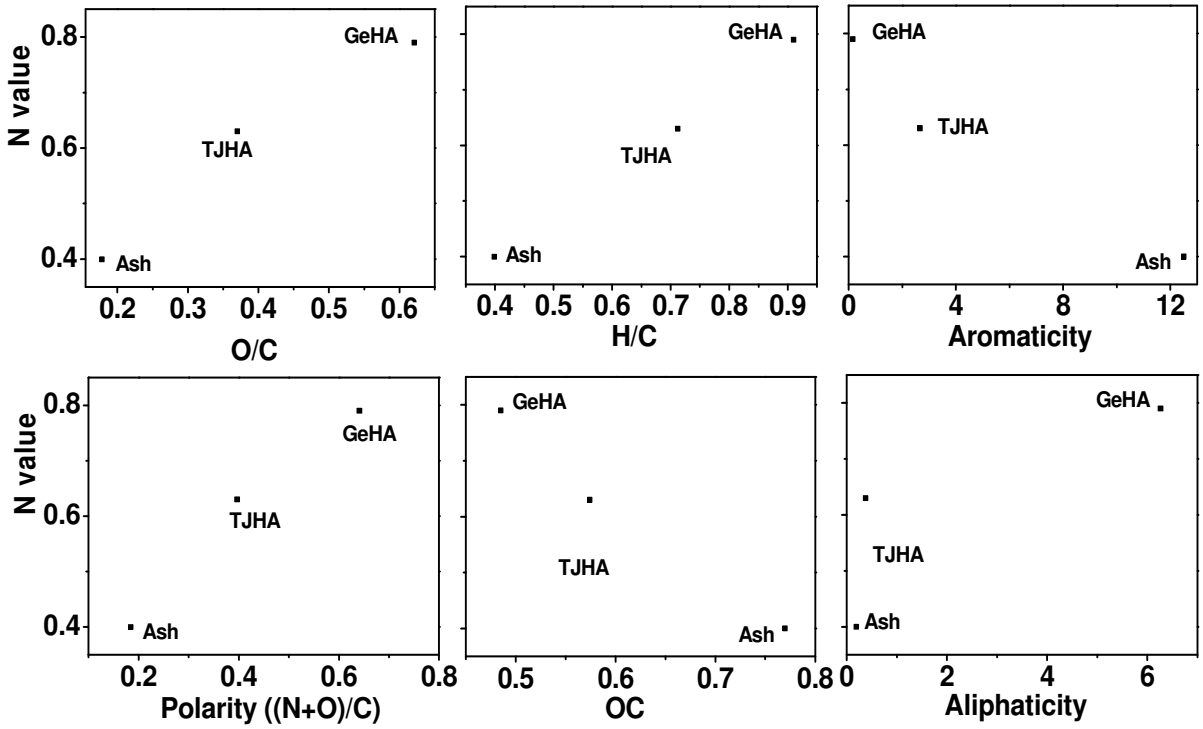

104

105 **FIGURE S1. Relationship between polarity ((N+O)/C and O/C ratio), or OC,**

106 **hydrophilicity (H/C ratio), aliphaticities (aliphatic C (0-110 ppm)/aromatic C**

107 **(110-165 ppm)), aromaticity of the adsorbents and N_s of TCP sorption.**

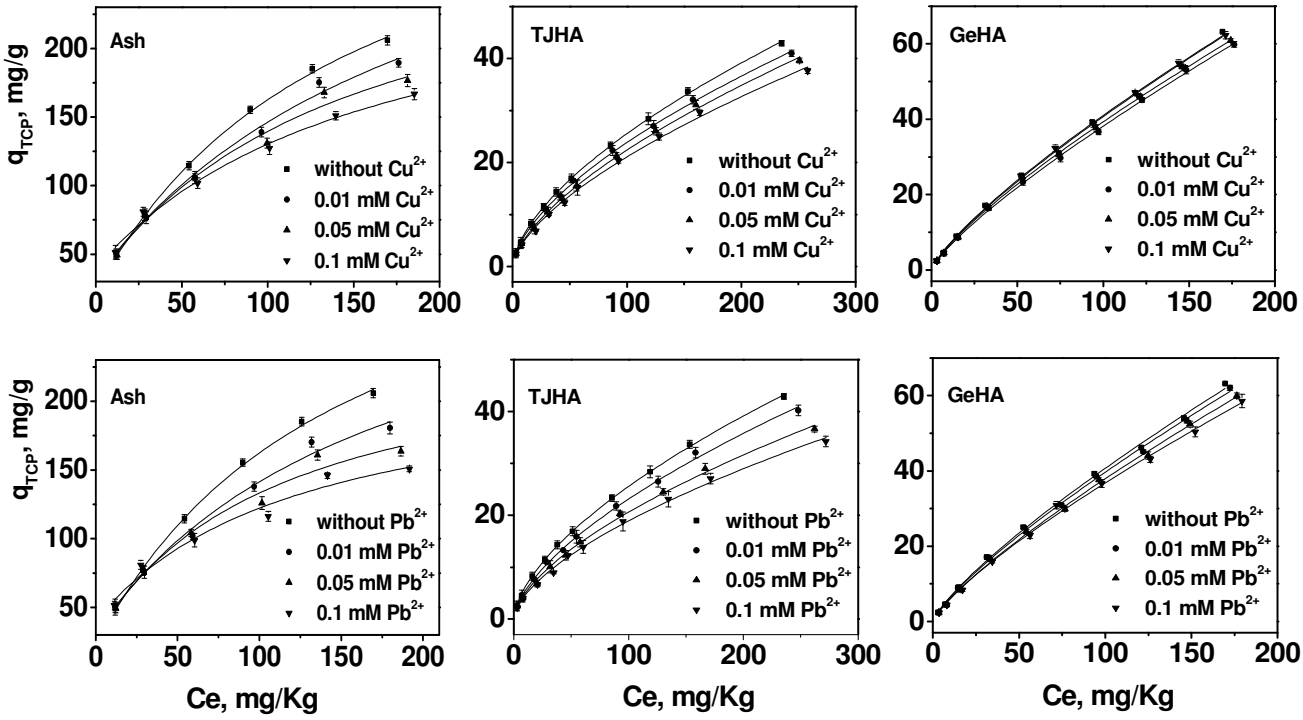

FIGURE S2. Effects of different initial concentrations of Cu^{2+} or Pb^{2+} on the sorption of TCP (q_{TCP}) (n = 3): (■) without Cu^{2+} or Pb^{2+}, (●) 0.01 mM, (▼) 0.05 mM, (▲) 0.1 mM Cu^{2+} or Pb^{2+}.

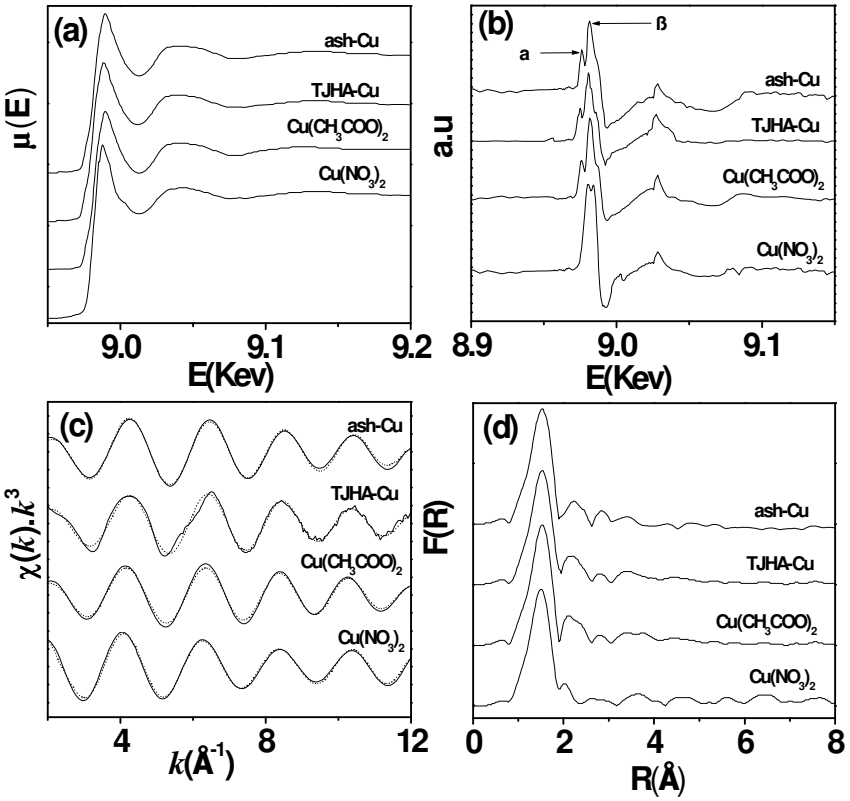

FIGURE S3. XAS spectra of Cu adsorbed-ash, -TJHA, -GeHA, and two reference compounds ($Cu(NO_3)_2$ and $Cu(CH_3COO)_2$): (a) normalized XANES spectra, (b) first derivative spectra, (c) raw and fitted EXAFS spectra (χ-function), (d) Fourier transformation of EXAFS spectra.

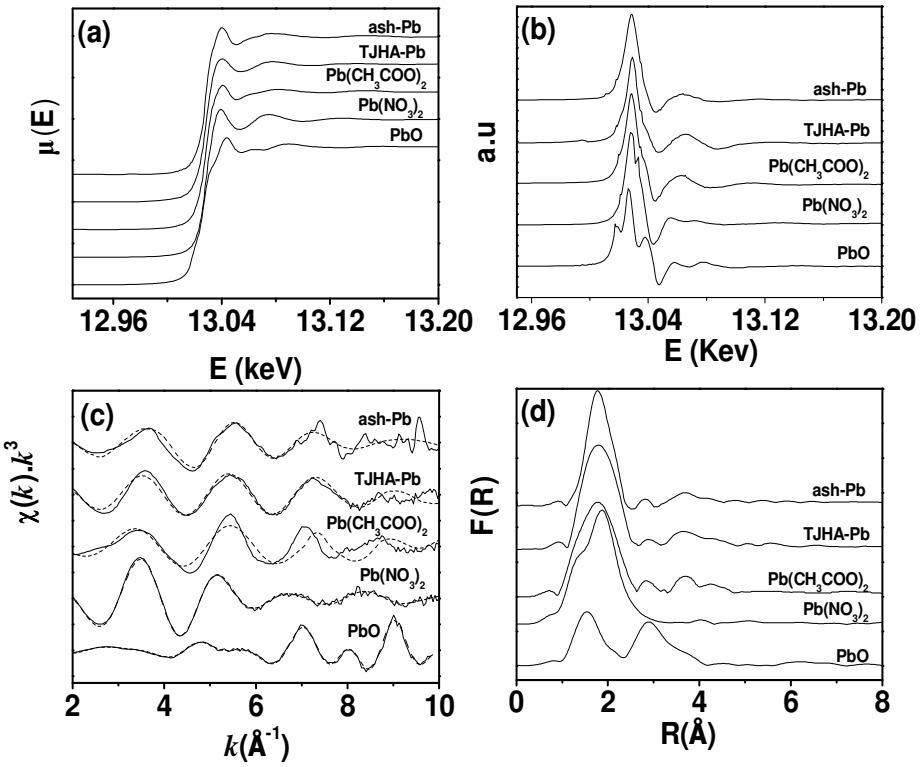

131

132 **FIGURE S4. XAS spectra of Pb adsorbed samples and reference compounds: (a)**

133 **normalized XANES spectra, (b) first derivatives, (c) raw and fitted EXAFS**

134 **spectra (χ-function), (d) Fourier transformation of EXAFS spectra.**

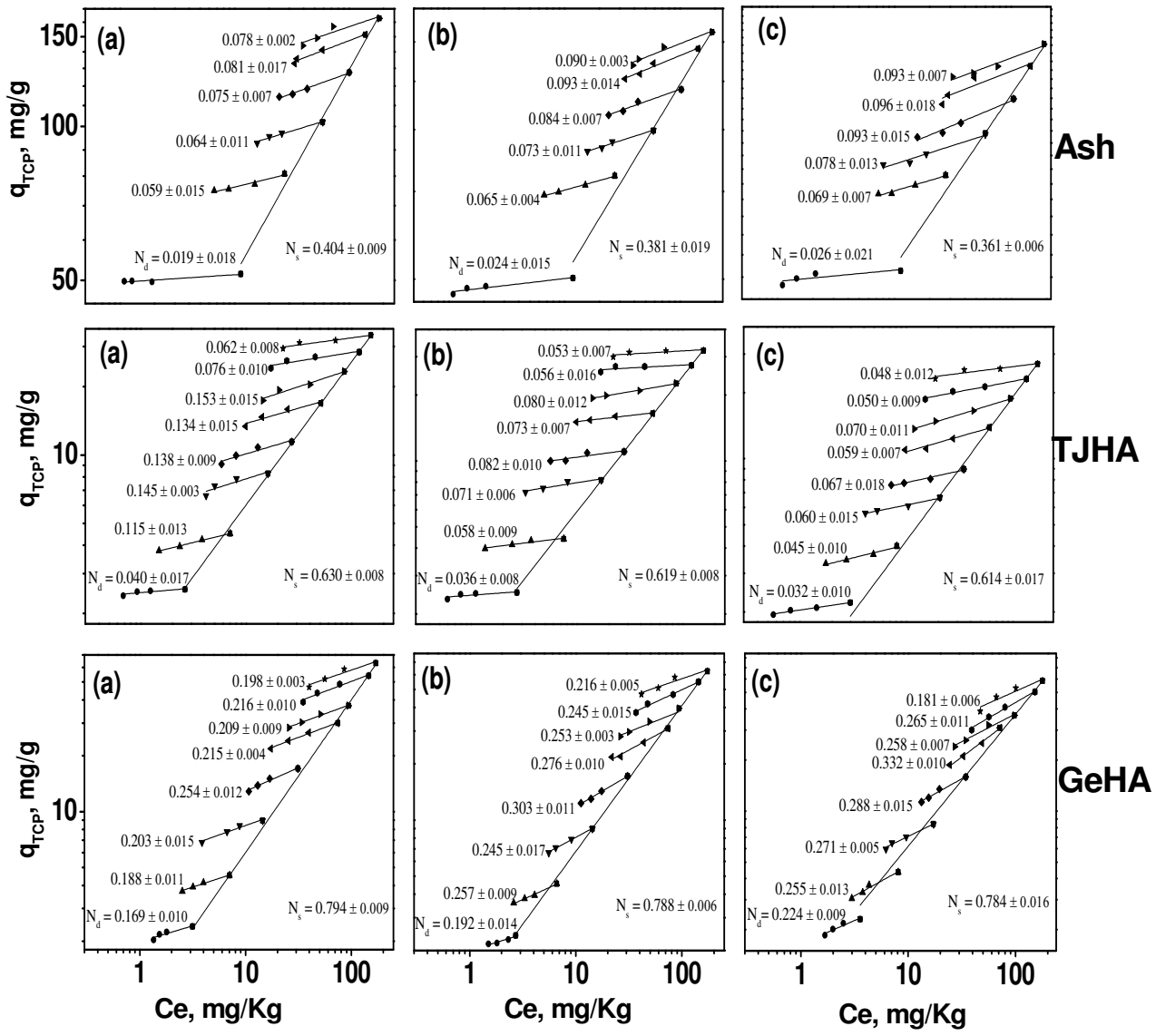

135

136 **FIGURE S5. Desorption of TCP in the absence of metals (a) and in the presence**

137 **of 0.1 mM Cu (b) or 0.1 mM Pb (c) (n = 3).**

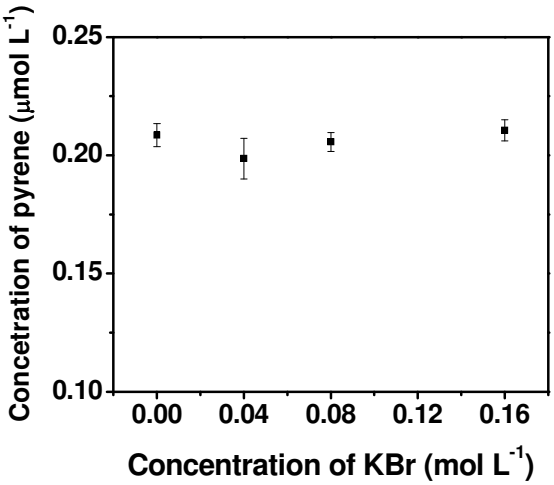

138

139 **FIGURE S6. Concentrations of pyrene (2.0×10^{-7} mol L^{-1}) (n = 4) in aqueous**

140 **solutions in the absence and presence of various concentrations of KBr.**

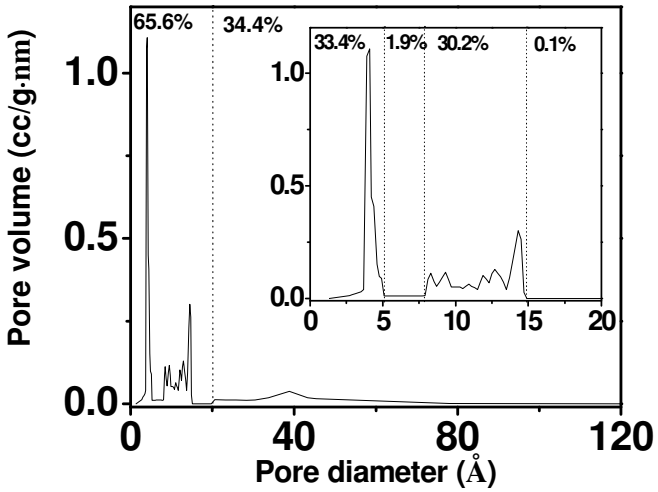

141

142 **FIGURE S7. Micropore diameter distribution of ash.**

143

144